The structure and luminescence properties of single-phase Sr_2YNbO_6: Bi^{3+}, Eu^{3+} tunable white light-emitting phosphors

JIA CHEN[2], JUN CHEN[1,*], MINGTAO WENG[2], JIEJIE WANG[2], XIAOYA XU[2], YIZHANG ZHUANG[2], XIAOQI CAI[2], XUHUI WU[2], SHAOJIAN WU[2], ZHIQIANG WU[2], YINSEN HUANG[2], JUNQIN FENG[1], DAOYUN ZHU[1], ZHONGFEI MU[1,*]

[1]*Experimental Teaching Department, Guangdong University of Technology, Waihuan Xi Road, No.100, Guangzhou 510006, PR China*

[2]*School of Materials and Energy, Guangdong University of Technology, Waihuan Xi Road, No.100, Guangzhou 510006, PR China*

A series of single-phase Sr_2YNbO_6(SYNO): Bi^{3+}, Eu^{3+} phosphors for light-emitting diode applications were synthesized by high-temperature solid state reactions. The XRD measurement indicated that the doping of Bi^{3+} and Eu^{3+} did not change crystal structure of the phosphors. The results show that the optimum doping concentrations of Bi^{3+} and Eu^{3+} ions are 0.03 and 0.12, respectively. The emission color of the SYNO: 0.03Bi^{3+}, 0.12Eu^{3+} phosphor can be adjusted from green to white to purple and blue by selecting appropriate excitation wavelengths in near-UV or the suitable Eu^{3+} doping contents. Especially, the white emission light is obtained when the excitation wavelength changes from 355 to 360 nm. All results indicate that Sr_2YNbO_6: Bi^{3+}, Eu^{3+} phosphor has a vast application prospect and preponderance in the field of white light-emitting diodes.

(Received December 15, 2022; accepted June 6, 2023)

Keywords: Sr_2YNbO_6: Bi^{3+}, Eu^{3+}, White light-emitting diodes, Phosphors

1. Introduction

White light-emitting diodes (w-LEDs) become a new type of solid lighting device in this century, exhibit great advantages such as small solid, shock resistant, not easy to damage, energy saving, high luminous efficiency, long life, no pollution, instantaneous start, no stroboscopic, etc. [1-7]. At present, there are three main methods for preparing w-LEDs: one is composed of blue LED chip and $Y_3Al_5O_{12}$: Ce^{3+} (YAG: Ce) phosphor. The second is to use UV and n-UV chips to excite three-color phosphors. And the third is three LED chips (red, green and blue) [8-12]. The shortcoming of first solution is the low color rendering index (CRI) [13-15], and the preparation of latter two solutions is complex and the cost is high. Using n-UV LED as excitation light source, a single-phase full-color white light emitting phosphor which not only can obtain good luminous effect, but also has the advantages of simple preparation and low cost. It is a promising method for the preparation of w- LED, and has become the research hotspot and frontier position.

In recent years, double perovskite niobate has become a research hotspot [16-22]. The electric dipole transition and the energy transfer (ET) will be strengthened due to the lower symmetry by stretching or twisting of the monoclinic crystal structure. There are a lot of related research reports here, such as $Ca_3MgSi_2O_8$:Eu^{3+}/Bi^{3+}, $Ba_3Y_4O_9$: Bi^{3+}/Eu^{3+}, Y_2GeO_5: Bi^{3+}/Eu^{3+}, $Ca_3Al_4ZnO_{10}$: Bi^{3+}/Mn^{4+} [23-28]. ET between Bi^{3+} ions and other dopant ions has been reported in these reports. In addition, some blue-green tunable phosphors have also been reported, such as $Ca_2Al_3O_6F$: Ce^{3+}, Tb^{3+}, $Ba_2Gd_2Si_4O_{13}$: Ce^{3+}, Tb^{3+} [29,30]. There are also related research reports on the adjustable color of light, for exampleY_2O_3: Bi^{3+}, Yb^{3+} [31,32]. However, there are very few experimental reports on Bi^{3+} and Eu^{3+} doped Sr_2YNbO_6. According to this manuscript, a kind of phosphor with adjustable color from blue and green to white phosphors by adjusting Eu^{3+} content or excitation wavelengths were synthesized. The luminescence mechanism of phosphors has been studied.

2. Experimental

A series of phosphors (Sr_2YNbO_6:$x$$Bi^{3+}$, x =0, 0.005, 0.01, 0.02, 0.03, 0.04, 0.05, and 0.075; Sr_2YNbO_6:0.03Bi^{3+}, $y$$Eu^{3+}$,$y$ = 0.02, 0.04, 0.06, 0.08, 0.10, 0.12, 0.14, 0.16, 0.18) were compounded through high temperature solid state way. This experiment are all using high-purity raw

materials of Y_2O_3 (Jining Tianyi New Materials Co., Ltd., 99.99%), $SrCO_3$ (Tianjin Kemiou Chemical Testing Co., Ltd., 99%), Nb_2O_5 (Aladdin, Shanghai Aladdin Industrial Co., Ltd., 99.9%), Bi_2O_3 (Tianjin Fuchen Chemical Testing Co., Ltd., 99%) and Eu_2O_3 (Aladdin, Shanghai Aladdin Industrial Co., Ltd., 99.99%). First, the powder was weighed, mixed and ground with a high-precision electronic scale in a certain proportion. The mixed powder was sintered at 1623 ℃ for 12 hours. And then it was ground and bagged to be tested after the sintered sample was naturally chilled to room temperature in air. According to this method, a series of samples were made and experiments were carried out.

The data of the XRD were measured by X-ray diffraction instrument. The microstructure image of the phosphors was collected by SEM. We use fluorescence spectrophotometer to record the emission and excitation spectra with the temperature-varying.

3. Results and discussion

3.1. Crystal structure and Composition

Structure details of Sr_2YNbO_6 are shown in Fig. 1. Sr_2YNbO_6 is a niobate with structure of double perovskite. The atoms of Nb, Sr and Y take shape together an octahedron with the oxygen atoms and its spatial group belongs to P21/n. Because the radii of Bi^{3+} (1.03 Å), Eu^{3+}(0.95 Å) is very similar to Y^{3+} (0.90 Å) [33], Bi^{3+} and Eu^{3+} ions are most likely to substitute Y^{3+} ions in Sr_2YNbO_6.

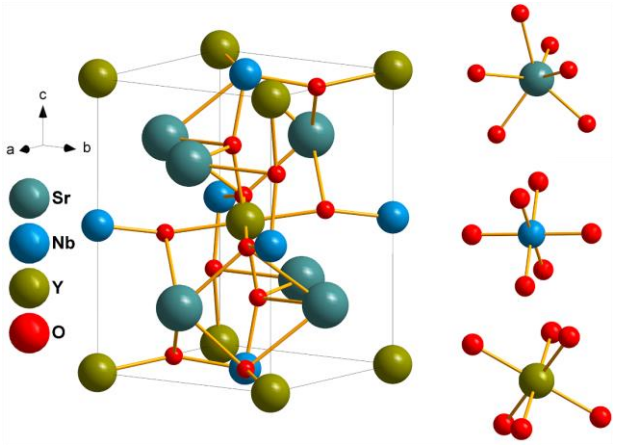

Fig. 1. Sr_2YNbO_6 structure diagram (color online)

Fig. 2(a) displays the XRD of series Sr_2YNbO_6 phosphors with undoped, doped Bi^{3+} ions, doped Eu^{3+} ions and Bi^{3+}/Eu^{3+} ions co-doping. XRD results showed that the peaks of diffraction in all phosphors is the same as the position identified by PDF#78-0537. Therefore, it can be seen that the above doping does not create an impurity phase in the samples. Fig. 2(b) shows the SEM of Sr_2YNbO_6:0.03Bi^{3+}. The appearance of agglomeration form is due to the typical characteristics of high temperature solid state method. These powders are relatively similar in size, between 2 and 8 μ m. This is beneficial to the luminescence of phosphors.

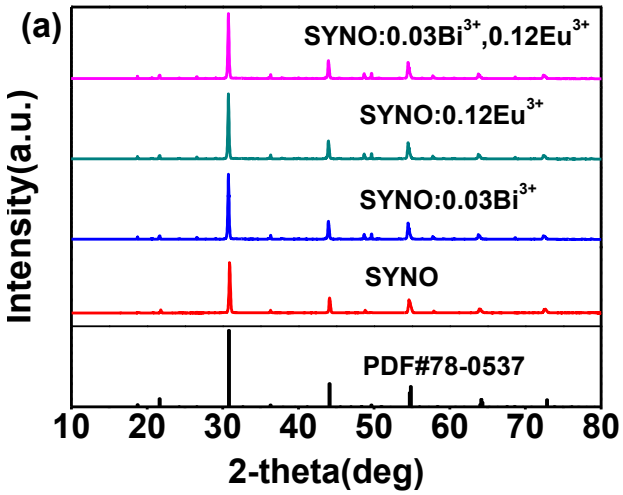

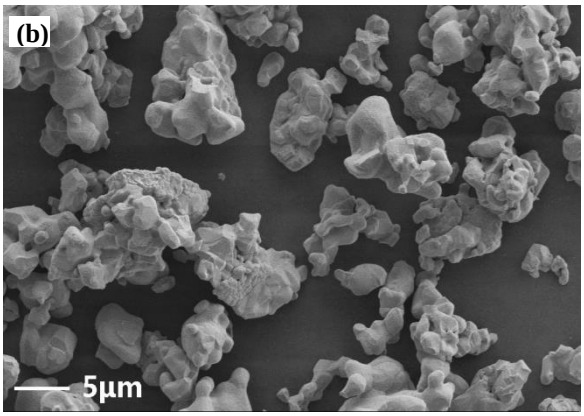

Fig. 2. (a) XRD image of Sr_2YNbO_6: xBi3+(x=0, 0.03), Sr_2YNbO_6:0.12Eu^{3+}, Sr_2YNbO_6:0.03Bi^{3+}, 0.12Eu^{3+} phosphors (color online) and (b) SEM of Sr_2YNbO_6: 0.03Bi^{3+}

3.2. Luminescence properties

Fig. 3 exhibits the emission of Sr_2YNbO_6: $x$$Bi^{3+}$ (x=0.005, 0.01, 0.02, 0.03, 0.04, 0.05, 0.075) that excited by 329 and 374 nm. It's obvious to see that the curve (329 nm excitation) has two broad bands Bi^{3+}(1)(507 nm) and Bi^{3+}(2)(419 nm) in Fig. 3(a), respectively. However, there is only one in Fig. 3(b), which is marked as Bi^{3+} (2) peaked of 419 nm (λ_{ex} = 374 nm). We found that the optimal doping concentration is 0.03, after which the emission intensity decreases rapidly due to the quenching effect.

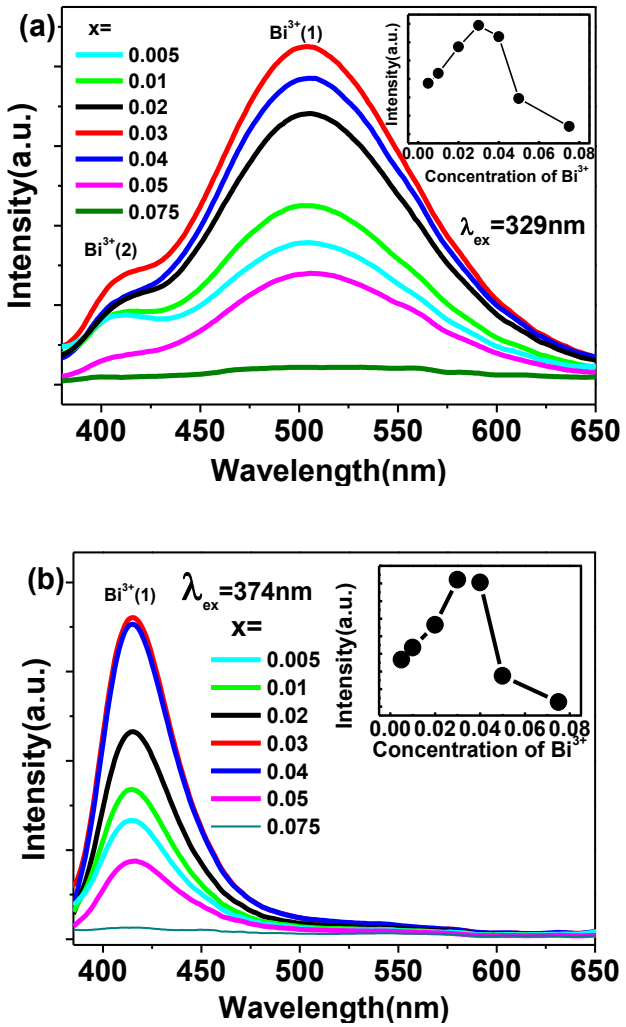

Fig. 3. PL spectra excited by (a) 329 nm and (b) 374 nm of Sr_2YNbO_6: xBi^{3+}(x=0.005, 0.01, 0.02, 0.03, 0.04, 0.05, 0.075) phosphors (color online)

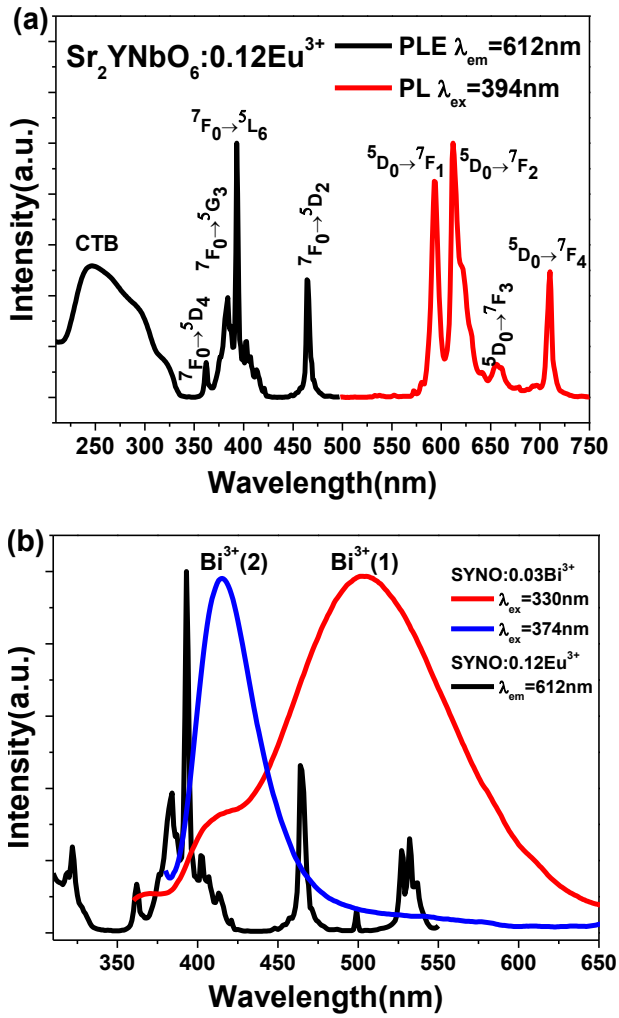

Fig. 4. (a) Emission and excitation curves of Sr_2YNbO_6: $0.12Eu^{3+}$ (b) the overlap between excitation spectra of Sr_2YNbO_6:$0.12Eu^{3+}$ and emission spectra of Sr_2YNbO_6:$0.03Bi^{3+}$ (color online)

In Fig. 4, PL and PLE spectra were placed together to facilitate comparative analysis. In PLE spectrum (monitoring 612 nm) of Fig. 4(a), the band in the range from 215 to 340 nm is allocated to charge transfer (CT) transitions [34,35]. Peaks at 362, 384, 393, and 465 nm are belong to $^7F_0 \rightarrow {}^5D_4$, $^7F_0 \rightarrow {}^5G_3$, $^7F_0 \rightarrow {}^5L_6$, $^7F_0 \rightarrow {}^5D_2$ transitions of Eu^{3+}, individually [36,37]. The PL spectrum at 394 nm shows the typical Eu^{3+} emission peaks of $^5D_0 \rightarrow {}^7F_J$ (J=0,1,2,3,4) transitions in the range of 560–720 nm [38,39]. It is greatly affected by the crystal environment, especially the position symmetry. Fig. 4(b) shows the emission spectra of Sr_2YNbO_6: $0.03Bi^{3+}$ (λ_{ex} are 329 nm and 374 nm) and the excitation spectra of Sr_2YNbO_6:$0.12Eu^{3+}$ (λ_{em}=613 nm). It is obvious that there is a great overlap from 375 nm to 550 nm between the broad emission peak of Bi^{3+} and the sharp PLE peak of Eu^{3+}, which indicates that ET occur between Bi^{3+} and Eu^{3+}.

Fig. 5(a) and (c) present the emission spectra of Sr_2YNbO_6: $0.03Bi^{3+}$, yEu^{3+}(y=0.02-0.18) under 329 nm and 374 nm excitation. It is obvious that the phosphors have not only the wide emission of Bi^{3+}, but also the linear peak emission of Eu^{3+}. The higher the content of Eu^{3+}, the weaker the emission intensity of Bi^{3+}. In contrast, the increase in Eu^{3+} content will increase the PL strength of the red components, reached the maximum at 0.12, and then decreased significantly because of the concentration quenching effect. The above results undoubtedly show that the red emission of Eu^{3+} in Sr_2YNbO_6: $0.03Bi^{3+}$, yEu^{3+} phosphors accompanied by the transfer of energy from Bi^{3+} to Eu^{3+}. The CIE of Sr_2YNbO_6:$0.03Bi^{3+}$, yEu^{3+} excited by 329 nm and 374 nm as shown in Fig. 5(b) and (d), respectively. Obviously, the CIE chromaticity coordinate (0.3166, 0.3688) in Fig. 5(b) shows that the white light is obtained. The luminous color changes from blue (0.1872, 0.0797) to red-purple (0.3003, 0.1728) in Fig. 5 (d) indicating that Sr_2YNbO_6: Bi^{3+}, Eu^{3+} phosphors can

convert n-UV light to suitable light source to promote plant photosynthesis.

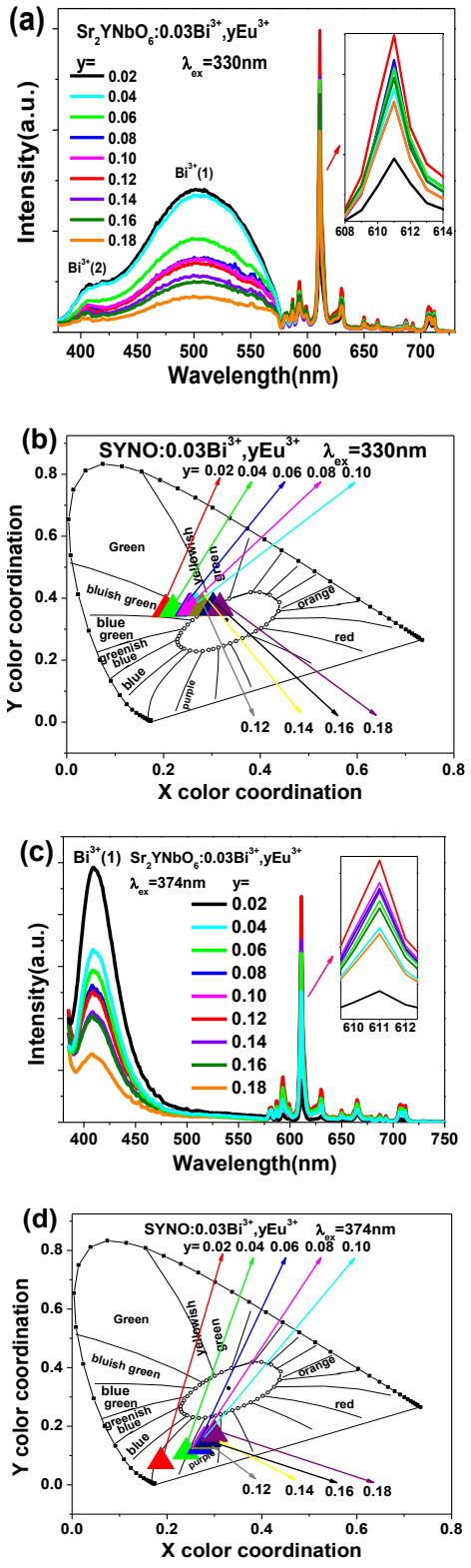

Fig. 5. Emission spectra (a) and CIE (b) under 329 nm excitation and emission spectra (c) and CIE (d) under 374 nm excitation of Sr_2YNbO_6: 0.03Bi^{3+}, yEu^{3+} (y = 0.02,0.04,0.06,0.08,0.10,0.12,0.14,0.16, 0.18) phosphors (color online)

The ET process between Bi^{3+} and Eu^{3+} could be explained by critical distance (*Rc*) [40]. *Rc* is represented by equation (1)

$$R_c = 2 \times \left[\frac{3V}{4\pi x_c N}\right]^{1/3} \quad (1)$$

where X_C represents the sum of the optimal doping concentration of Bi^{3+} and Eu^{3+} ions, *V* stands for the volume of unit cell, *N* stands for the sites number. X_C = 0.15, *V*=281.02 Å^3, *N* = 2. According to the calculation of equation (1), *Rc* equals 12.14 Å. Therefore, multipole interaction is the major ET mechanism of concentration quenching effect. According to Dexiter's theory [41], the specific form of interaction is given by equation (2):

$$\frac{\eta_0}{\eta_s} \approx \frac{I_0}{I_x} \propto C^{\frac{n}{3}} \quad (2)$$

In Eq.(2), I_0/I_x can be approximately used instead of the η_0/η_s. The emission intensities of Bi^{3+} are I_0 and I_x for the doped and undoped Eu^{3+} ions, respectively. The total doping concentration of Bi^{3+} and Eu^{3+} is *C*. The *n* value presents different interaction types that including 3, 6, 8, and 10. The Fig. 6 matched I_0/I_x with $C^{n/3}$ by linear function. It indicates that the major ET mechanism in Sr_2YNbO_6: Bi^{3+}, Eu^{3+} is quadrupole-quadrupole (q-q) interaction.

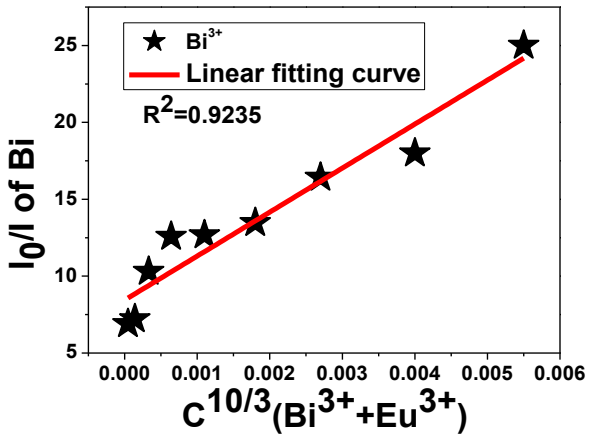

Fig. 6. Dependences of (I_0/I) of Bi^{3+} and Bi^{3+}+Ei^{3+} on $C^{10/3}$ (color online)

Fig. 7(a) shows the emission spectra for Sr_2YNbO_6: 0.03Bi^{3+}, 0.12Eu^{3+} under 329 to 374 nm excitation. Remarkably, as the wavelength of excitation increases, the PL emission position of the Bi^{3+} and Eu^{3+} remains unchanged, but the luminous intensity changes. Therefore, blue, green and red luminescence is realized by different excitation wavelengths. The International Commission on illumination (CIE) chromaticity coordinates of Sr_2YNbO_6: 0.03Bi^{3+}, 0.12Eu^{3+} excited by different wavelengths light

is shown in Fig. 7(b). It is obvious that the emission color of the Sr_2YNbO_6: $0.03Bi^{3+}$, $0.12Eu^{3+}$ phosphor can be adjusted from green to white to purple. Especially, the white emission light is obtained when the excitation wavelength changes from 355 to 360 nm. According to this, the emission spectra of Sr_2YNbO_6:Bi^{3+}, Eu^{3+} can be regulated by choosing fitting excitation wavelength in close to UV. It has a peculiarly significant for implementation in simple-phase w-LEDs.

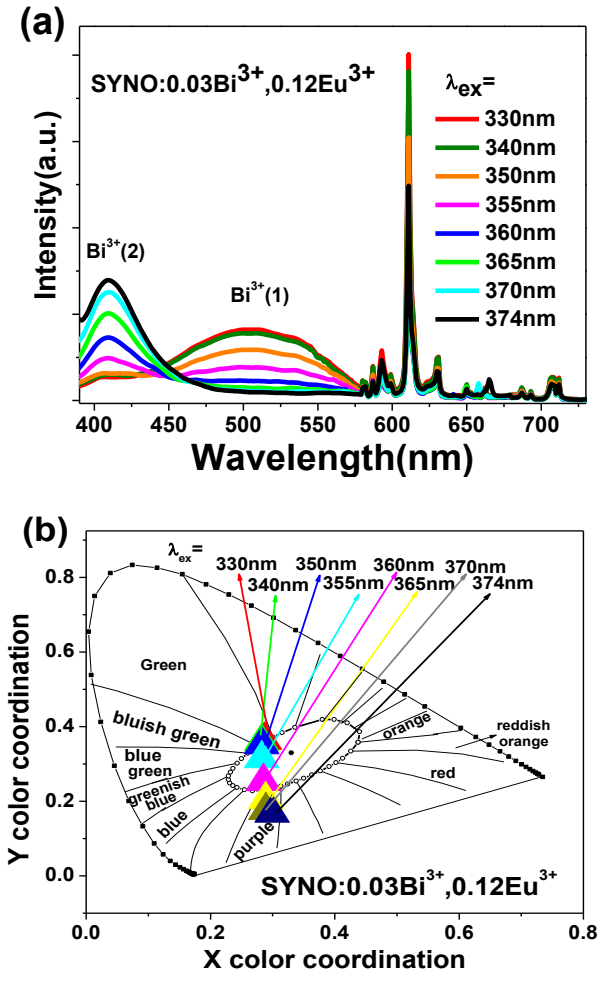

Fig. 7. (a) Emission spectra and (b) CIE chromaticity coordinates of Sr_2YNbO_6: $0.03Bi^{3+}$, $0.12Eu^{3+}$ with various excitation light from 329 nm to 374 nm (color online)

The emission spectra of Sr_2YNbO_6: $0.03Bi^{3+}$, $0.12Eu^{3+}$ at 329 nm excitation wavelength in diffierent temperature ranges from 298 to 548 K are shown in Fig. 8. The PL intensity of Bi^{3+} and Eu^{3+} decreases monotonically and slowly as the temperature increases from 298 K to 548 K. The pattern and state of the curves do not change. Therefore, the temperature quenching is observed. At the point when the temperature comes to 448 K, the intensity maintain at 53.04% of that at 298 K (room temperature) for Bi^{3+} and 30.39% for Eu^{3+} (see inset in Fig. 8). Sr_2YNbO_6: Bi^{3+}, Eu^{3+} single-phase color-modulated phosphors with excellent properties were prepared.

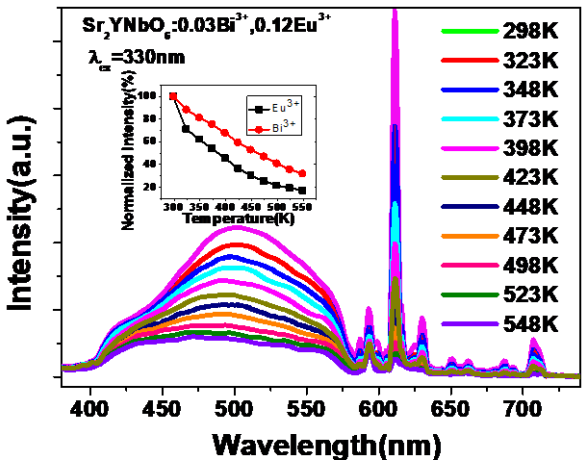

Fig. 8. The temperature-varying emission spectra (λ_{ex} = 329 nm) of Sr_2YNbO_6: $0.03Bi^{3+}$, $0.12Eu^{3+}$, the inset shows normalized integrated emission intensity of Bi^{3+} and Eu^{3+} versus temperature (color online)

4. Conclusions

The crystal structure of Sr_2YNbO_6 is not affected by the different consistencies of Bi^{3+} and Eu^{3+} doping. The PL spectrum of Sr_2YNbO_6: xBi^{3+} (x=0.005-0.075) phosphors contain two wideband emission spectrum spikes at 419 nm (Bi^{3+} (2)) and 507 nm (Bi^{3+} (1)), separately. The ideal doping convergence of Bi^{3+} and Eu^{3+} particies are 0.03 and 0.12, respectively. Some of this ET is migrated from Bi^{3+} (1) and Bi^{3+} (2) sites to Eu^{3+} ion was observed. Under the excitation of 329 nm and 374 nm, emission spectra from green to white and blue to purple can be acquired by changing the substance of Eu^{3+}. Moveover, the CIE shows that the luminous color of Sr_2YNbO_6: $0.03Bi^{3+}$, $0.12Eu^{3+}$ phosphor could be altered from green to white and later to purple under various excitation frequency from 329 nm to 374 nm. Increased temperature leads to reduced emission intensity (298–548 K) which displays the unique thermal quenching behavior. The PL intensity at 448 K remain at 53.04% of that at 298 K (room temperature) for Bi^{3+} and 30.39% for Eu^{3+}. Hence, Sr_2YNbO_6:Bi^{3+}, Eu^{3+} phosphors can still maintain excellent stability at different temperatures. Summarizing all the above results, it can be clearly concluded that Sr_2YNbO_6: Bi^{3+}, Eu^{3+} phosphor is a useful candidate material in the field of single-phase white LED.

Acknowledgements

This work was supported in part by the National Natural Science Foundation of China (Grant No. 52272142, 62127816), in part by the Science and Technology Program of Guangzhou, China (Grant No.

202102080261, 202002030091), in part by the National Key R&D Program of China (Grant No. 2018YFB1801001), in part by the Guangdong Introducing Innovative and Enterpreneurial Teams of "The Pearl River Talent Recruitment Program" (Grant No. 2019ZT08X340), in part by the Research and Development Plan in Key Areas of Guangdong Province (Grant No. 2018B010114002). Authors also thank the test support from the Shiyanjia lab (www.shiyanjia.com).

References

[1] P. Du, X. Y. Huang, J. S. Yu, Chem. Eng. J. **337**, 91 (2018).
[2] H. Guo, X. Y. Huang, Y. J. Zeng, J. Alloys Compd. **741**, 300 (2018).
[3] S. C. Hou, M. K. Gangishetty, Q. M. Quan, D. N. Congreve, Joule **2**, 2421 (2018).
[4] Z. He, M. Gao, L. Zhuo, K. Yang, L. Lv, S. Chen, Y. Pan, Mater. Res. Bull. 1**56**, 111994 (2022).
[5] X. Liu, W. Zhang, R. Xu, J. Tu, G. Fang, Y. Pan, Dalton Trans. **51**, 10029 (2022).
[6] M. Xie, G. Zhu, W. Xie, D. Li, X. Zhou, Optoelectron. Adv. Mat. **11**, 32 (2017).
[7] H. Zhu, C. Peng, J. Li, X. Cao, Y. Pan, J. Lumin. **252**, 119321 (2022).
[8] P. F. S. Pereira, M. G. Matos, L. R. Avila, E. C. O. Nassor, A. Cestari, K. J. Ciuffi, P. S. Calefi, E. J. Nassar, J. Lumin. **130**, 488 (2010).
[9] Y. Q. Wang, Y. G. Wang, N. Chi, J. J. Yu, H. L. Shang, Opt. Express **21**, 1203 (2013).
[10] R. Cao, H. Liang, T. Chen, Z. Wu, Z. Jiang, X. Yi, J. Wen, Q. Zhong, J. Phys. Chem. Solids **163**, 110569 (2022).
[11] R. Cao, Y. Ye, Q. Peng, S. Guo, Z. Hu, W. Hu, H. Ao, X. Yu, Optoelectron. Adv. Mat. **12**(1-2), 71 (2018).
[12] R. Cao, Y. Zhao, Z. Hu, W. Shao, F. Xiao, G. Zheng, P. Liu, T. Chen, J. Lumin. **238**, 118248 (2021).
[13] A. Aboulaich, M. Michalska, R. Schneider, A. Potdevin, J. Deschamps, R. Deloncle, G. Chadeyron, R. Mahiou, ACS Appl. Mater. Interfaces **6**, 252 (2014).
[14] V. Bachmann, C. Ronda, A. Meijerink, Chem. Mat. **21**, 2077 (2009).
[15] R. Cao, Z. Jiang, T. Chen, H. Liang, X. Yi, Y. Zhong, H. Zhang, W. Luo, J. Lumin. **243**, 118618 (2022).
[16] J. Chen, S. Zhao, Z. Zhao, M. Liao, S. Pan, J. Feng, D. Zhu, W. Pang, J. Lin, Z. Mu, J. Lumin. **239**, 118336 (2021).
[17] A. Fu, C. Y. Zhou, Q. Chen, Z. Z. Lu, T. J. Huang, H. Wang, L. Y. Zhou, Ceram. Int. **43**, 6353 (2017).
[18] Z. Z. Lu, T. J. Huang, R. P. Deng, H. Wang, L. L. Wen, M. X. Huang, L. Y. Zhou, C. Y. Yao, Superlattices Microstruct. **117**, 476 (2018).
[19] W. Ruan, M. Xie, Q. Yang, L. Hu, K. Su, Inorg. Chem. Front. **9**, 5267 (2022).
[20] W. Ruan, R. Zhang, Q. Zhong, Y. Fu, Z. Yang, M. Xie, RSC Adv. **12**, 14819 (2022).
[21] M. Xie, W. Ruan, J. Wang, J. Lumin. **224**, 117278 (2020).
[22] M. Xie, J. Wang, W. Ruan, J. Lumin. **218**, 116848 (2020).
[23] K. Li, Hz. Lian, M. Shang, J. Lin, Dalton Trans. **44**, 20542 (2015).
[24] Z. H. Sun, M. Q. Wang, Z. Yang, K. P. Liu, F. Y. Zhu, J. Solid State Chem. 2**39**, 165 (2016).
[25] W. Y. Zhao, S. M. Qi, J. Liu, B. Fan, J. Alloys Compd. **787**, 469 (2019).
[26] Z. Zhou, Y. Zhong, M. Xia, N. Zhou, B. F. Lei, J. Wang, F. F. Wu, J. Mater. Chem. C. **6**, 8914 (2018).
[27] R. Cao, N. Liu, Q. Zhong, Y. Tu, Y. Xu, H. Zhang, W. Luo, T. Chen, J. Mater. Sci. Mater. Electron. **32**, 26620 (2021).
[28] M. Gao, W. Zhang, B. Wu, Y. Dai, C. Peng, Y. Pan, J. Lumin. **249**, 119011 (2022).
[29] H. Guo, H. Zhang, J. J. Li, F. Li, Opt. Express **18**, 27257 (2010).
[30] Z. G. Xia, R.-S. Liu, J. Phys. Chem. C **116**, 15604 (2012).
[31] X. Y. Huang, X. H. Ji, Q. Y. Zhang, J. Am. Ceram. Soc. **94**, 833 (2011).
[32] R. M. Jafer, E. Coetsee, A. Yousif, R. E. Kroon, O. M. Ntwaeaborwa, H. C. Swart, Appl. Surf. Sci. **332**, 198 (2015).
[33] C. J. Howard, P. W. Barnes, B. J. Kennedy, P. M. Woodward, Acta Crystallogr. Sect. B: Struct. Sci. **61**, 258 (2005).
[34] D. M. D'Alessandro, F. R. Keene, Chem. Soc. Rev. **35**, 424 (2006).
[35] S. Johnston, A. Mukherjee, I. Elfimov, M. Berciu, G. A. Sawatzky, Phys. Rev. Lett. **112**, 5 (2014).
[36] L. Li, W. X. Chang, W. Y. Chen, Z. S. Feng, C. L. Zhao, P. F. Jiang, Y. J. Wang, X. J. Zhou, A. Suchocki, Ceram. Int. **43**, 2720 (2017).
[37] Q. Liu, X. B. Li, B. Zhang, L. X. Wang, Q. T. Zhang, L. Zhang, Ceram. Int. **42**, 15294 (2016).
[38] F. Y. Fan, L. Zhao, Y. F. Shang, J. Liu, W. B. Chen, Y. Y. Li, J. Lumin. **211**, 14 (2019).
[39] J. S. Zhong, H. B. Gao, Y. J. Yuan, L. F. Chen, D. Q. Chen, Z. G. Ji, J. Alloys Compd. **735**, 2303 (2018).
[40] L. G. Van Uitert, J. Electrochem. Soc. **114**, 1048 (1967).
[41] G. Blasse, Phys. Lett. A. **28**, 444 (1968).

*Corresponding author: chenjun@gdut.edu.cn;
muzhongfei@gdut.edu.cn